ELSEVIER

Thermochimica Acta 302 (1997) 25–34

thermochimica acta

Hydration kinetics of $CaAl_2O_4$ using synchrotron energy-dispersive diffraction

Shahwana Rashid[a], Xavier Turrillas[b,*]

[a] *Lafarge Aluminates, 730, London Road, Grays, Essex RM20 3NJ, UK*

[b] *Instituto de Ciencias de la Construcción Eduardo Torroja, Consejo Superior de Investigaciones Científicas; Serrano Galvache s/n, 28033 Madrid, Spain*

Received 10 January 1997

Abstract

Synchrotron energy-dispersive diffraction has been employed to monitor the hydration of $CaAl_2O_4$. Diffraction intensities of neat pastes, with a water-to-solid ratio (w/s) of 0.4, were employed to follow the hydration progress at temperatures ranging from 60°C to 90°C. The hydration rate of $CaAl_2O_4$ increased with temperature according to a three-dimensional diffusion-controlled model expressed by $[1-(1-\alpha)^{1/3}]^2 = kt$, with reaction constants k ranging from 7.4×10^{-1} min^{-1} at 70°C to 3.2×10^{-2} min^{-1} at 90°C. The activation energy was 84 kJ mol^{-1} K^{-1}. The onset of $Ca_3Al_2O_6.6H_2O$ diffraction peaks from $CaAl_2O_4$, at 90°C, was within 3 min whereas at 60°C it was after 8 min. The results show that $Ca_2Al_2O_5.8H_2O$ is the intermediate in the hydration of $CaAl_2O_4$ to $Ca_3Al_2O_6.6H_2O$, in all cases. The hydration is explained in solid-state kinetics terms, $Ca_2Al_2O_5.8H_2O$ playing a key rôle in $CaAl_2O_4$ hydration for triggering the hydration to form $Ca_3Al_2O_6.6H_2O$.

Keywords: Calcium aluminate; Hydration; Kinetics; Synchrotron radiation; Time-resolved energy-dispersive diffraction

1. Introduction

Conventional powder X-ray diffraction in time- and/or temperature-resolved mode is an experimental technique well established to study solid-state kinetics of crystalline materials. There are many publications on this subject but only one will be mentioned as a recent illustrative example [1].

On the other hand, the validity of synchrotron energy-dispersive diffraction (EDD) has been used to monitor in situ, bulk samples while hydrating, especially at temperatures over 50°C. However, the real potential of this powerful state-of-the-art technique has yet to be fully appreciated as presently mainly qualitative results [2] have been published although accurate quantitative analyses can also be achieved.

Monocalcium aluminate (CA[1]) has been the focus of much research though by no means has the study reached the status of complete understanding. A recent research publication gives an up-to-date picture of the knowledge on this topic [3].

Standard literature states that at higher temperatures (above 28°C) in the presence of water, CA forms the stable cubic hydrate C_3AH_6 according to the following equation [4];

$$3CA + 12H \rightarrow C_3AH_6 + 2AH_3, \quad (1)$$

*Corresponding author. Tel.: 00 34 1 302 0440; fax: 00 34 1 302 0700; e-mail: xtx@xrdsv1.dl.ac.uk.

[1] A special shorthand notation known as cement chemists notation is used to simplify formulae and is as follows; C≡CaO, A≡Al_2O_3, S≡SiO2, F≡Fe_2O_3, H≡H_2O, $\bar{S} \equiv SO_3$, $\bar{C} \equiv CO_3$, M≡MgO, T≡TiO

0040-6031/97/$17.00
PII S0040-6031(97)00216-5

and that the metastable hydrate C_2AH_8 is also formed at these temperatures according to Eq. (2);

$$2CA + 11H \rightarrow C_2AH_8 + AH_3 \quad (2)$$

and above 50°C only the reaction in Eq. (1) occurs, although this last statement has been recently proved to be inexact, using other experimental techniques as it will be shown below.

It is perhaps pertinent to briefly introduce the original conclusion, since the hydration of CA, above 50°C, was made. The majority of the fundamental knowledge on calcium aluminates has arisen from solution chemistry following the solubility of the various phases under dilute solutions (water-to-solid ratio 10 : 1). These studies have proved extremely informative in our understanding of such complicated systems; nevertheless they have been limited by the static nature of the procedure. The rapidly changing calcium aluminate systems, specially at higher temperatures were not appropriately studied using an experimental technique capable of discerning fast phase transitions.

The initial realisation that there might be other reactions occurring at higher temperatures was highlighted by Rettel et al. [5] utilising NMR methods. Clearly from their results it was seen that the formation of C_3AH_6 was accompanied by C_2AH_8, although the precise details of the reaction could not be appreciated with this technique alone.

However as calcium aluminates and their products have the advantage of being relatively crystalline, they can more readily be monitored with diffraction techniques. With the advent of the state-of-the-art diffraction methods, such as EDD, it is possible to study continuously changing systems without the restrictions of conventional X-ray diffraction regarding the state of the sample and environmental conditions. Suspensions of solids in water in transmission mode can be irradiated with a white synchrotron beam and a number of diffraction reflections at a fixed 2θ angle, simultaneously collected. This allows for fast data capture and for the study of fast phase transitions even under non-standard temperature/pressure conditions.

In doing so it has been possible, not only to confirm the presence of C_2AH_8 at temperatures above 50°C, but also show that it plays quite an important rôle in the hydration of CA. It has been reported that it is in fact a nucleating trigger for the formation of C_3AH_6 [6].

The studies undertaken here will confirm this hypothesis and also show that the hydration is in fact governed, not by a through-solution mechanism but more so by a solid-state mechanism.

2. Materials and experimental procedure

2.1. Materials

The samples of monocalcium aluminate, provided by Lafarge Central Laboratory, France, were prepared by firing calcium carbonate ($CaCO_3$) with α-alumina, twice, approximately at temperatures of 1500°C and 1530°C. They were then ground to a blaine fineness of approx. 0.30 m^2/g [7]. The particle size distribution profile was obtained using a laser granulometer of Malvern Instruments. The size distribution curve presented a maximum frequency for 22.8 μm with 90% of the particles lower than 87 μm and 10% lower than 7.5 μm. The specific surface area amounted to 0.39 m^2/g.

The purity was checked by conventional X-ray diffraction which showed only reflections corresponding to the orthorhombic phase ($CaAl_2O_4$.)

2.2. Apparatus

2.2.1. Synchrotron source

Station 9.7, operating in EDD mode, at the Synchrotron Radiation Source in Daresbury Laboratory (UK) was used to study the hydration of CA at varying temperatures ranging from 60°C to 90°C. A schematic set-up of the station is illustrated in Fig. 1.

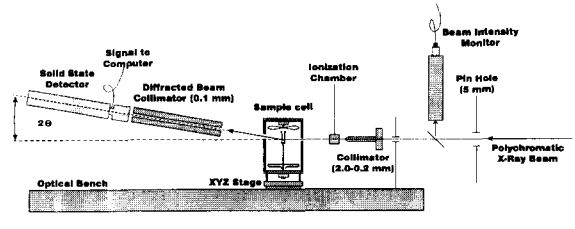

Fig. 1. Schematic set-up for energy-dispersive diffraction at station 9.7, Daresbury Laboratory.

The station receives white radiation directly from a 5T *wiggler*. The beam, passing through a water-cooled aperture and a pinhole for collimation, was further collimated by a set of slits. It then passed through a fine beryllium window before it reached the sample stage where it travelled through the sample and was channelled, with two molybdenum parallel plates, to the fixed solid-state detector.

The solid-state energy-sensitive detector was cooled with liquid nitrogen and coupled to a multichannel analyser (MCA) which was capable of discriminating the incident photons according to their energy. The MCA consisted of a highly pure germanium crystal using reverse bias p–n junctions as the detecting elements. Its saturation threshold was only 40 kcps and precautions were taken not to exceed this limit hence preventing distortion of the diffracted output.

The goniometer angle was predetermined at a fixed angle of around 3° 2θ. The diffraction pattern covered a range of approximately 5 keV to 60 keV, which is equivalent to a usable region in *d*-spacings of 12 Å to 3 Å. Most of the phases of interest exhibit distinctive reflections in this region hence allowing for their identification and surveillance. More details about the set-up of the ancillary can be found in Clark [8].

2.2.2. Environmental cell

The sample holders used were fabricated from PEEK (polyaryletheretherketone), a polymer chosen because of its resistance to high pH and low X-ray absorption. The sample holders were cylindrical in shape ≈6 mm in diameter and 20 mm in height and were equipped with stainless steel lids with rubber o-rings ensuring air tightness.

The PEEK container was housed in a cylindrical furnace containing a heating element at the bottom and a rotating fan at the top which ensured homogeneous temperature within the furnace. Any thermal losses were minimised by the double metallic wall separated by a layer of insulating material.

The container was placed on top of a spindle, in the middle of the furnace, connected to a motor rotating at a speed of 3 rpm. This dampened any effects of preferred orientation.

A single thermocouple, attached to the metallic lid of the sample holder, measured and controlled the temperature and power delivered to the heating element. Both the heating element and the K-type thermocouple were connected to an Omega RA 457 temperature controller, working with an appreciation of ±0.1°C.

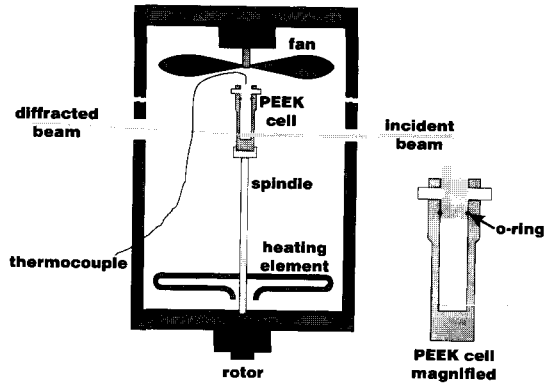

Fig. 2. The Schlumberger furnace used for hydration under hydrothermal conditions, showing the main features: heating element, fan, thermocouple and PEEK cell.

Two holes, on either side of the furnace, allowed the passage of the beam to and from the sample. A schematic representation of the Schlumberger furnace is given in Fig. 2.

2.2.3. Experimental procedure

Approximately 2 g of CA was hand mixed to a paste with 0.8 gms of deionised and CO_2-free water, maintaining a water-to-solid (w/s) ratio of 0.4, and immediately transferred to the PEEK cell. This was then carefully introduced in the furnace held at the appropriate temperature. The diffracting volume was estimated to be 1 mg (considered from the goniometer angle and the collimators) within the bulk of the sample and statistically represented.

In all the experiments the data collection commenced approximately 1 min after mixing.

The hydration was monitored at interval of 15 s for the temperatures ranging from 80°C to 90°C. While at 70°C the data were collected every 30 s and at 60°C it was every minute.

The hydration kinetics of the reaction was monitored by following the (211) diffraction reflection corresponding to the hydrate product C_3AH_6.

2.2.4. Treatment of the data

The raw diffraction data were accommodated by various in-house developed programs [9,10] and a commercial package UNIRAS/UNIMAP (version 6) which was used for the three- and two-dimensional topographic diagrams.

The peak intensities were calculated by simple integration applying the Simpson rule (adding the photon counts under the peaks). Normalised intensities were corrected subtracting the averaged background and this evolution with time was complied with the commercial software package ORIGIN [11]. In addition various fittings to kinetics models were performed with this package which employs a non-linear least squares algorithm (Levenberg–Marquardt's).

The kinetics of the reaction were represented in the conventional manner of plotting the reaction rate (α) versus reduced time. The reaction rate was determined by normalising the peak intensities (i.e. $\alpha = 1$ when reaction was completed). For the reduced time scale transformation, an arbitrary value of 1 was given when the reaction rate was 0.9.

3. Results

The hydration of CA was followed by the sequential acquisition of diffraction patterns at regular intervals. Variations in peak intensities and positions were associated with the consumption and synthesis of the crystalline phases during the reaction. Pseudo-three-dimensional representation (juxtaposing the individual diffraction patterns in a time sequence) and corresponding two-dimensional contour maps (associated topographic contour maps) were primarily used to give a general global perspective and history of the events that took place during the experiment.

The x-axis is converted into the inverse of d-spacing (more exactly 1000/d) to prevent any distortion of the diffraction peaks. The y-axis represents the reaction time, expressed in minutes in most the cases. The x-axis displays the relative intensities given by the total count of photons (reduced to the number of counts per second in most cases) recorded by the energy detector.

Fig. 3 shows the hydration of CA at 90°C. The hydration, at the varying temperatures, shows very similar trends; the main constituent CA hydrating to C_3AH_6, AH_3 (gibbsite) and C_2AH_8 which forms as an intermediate phase.

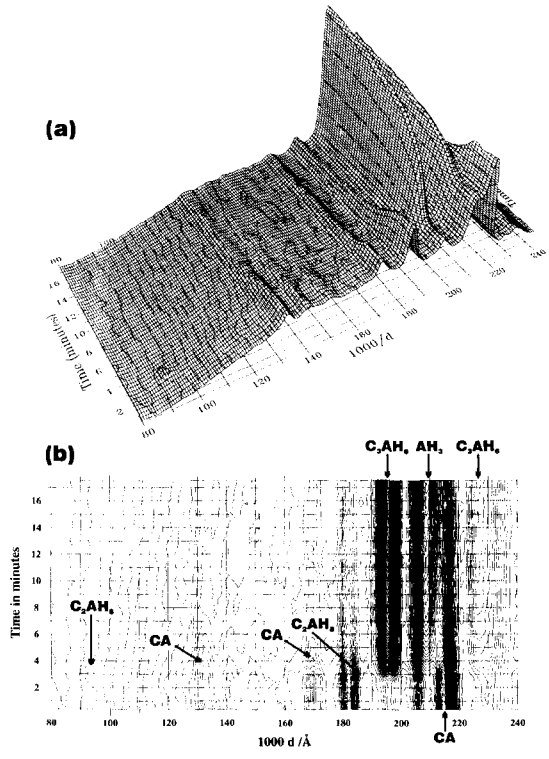

Fig. 3. Hydration of CA at 90°C, with time, using synchrotron energy-dispersive diffraction. CA transforms to C_3AH_6 with C_2AH_8 as an intermediary phase. (a) the three-dimensional time resolved diagram, (b) the corresponding two-dimensional diagram.

A common feature observed in the hydration, throughout the different temperatures, is that C_2AH_8 doubtlessly emerges as a transient phase. Furthermore, a slight increase in the background is discerned accompanying C_2AH_8, which is attributed to the formation of alumina gel. This eventually crystallises to gibbsite (AH_3).

A point of interest which has arisen from these studies is the polymorphic nature of C_2AH_8. It was found, while computing the individual peak intensities of the phases, that both the α and β forms of C_2AH_8 were present. The splitting was observed in the main two reflections; (001) and (002). In order to confirm this observation, conventional X-ray diffraction, at 60°C was undertaken. It was verified that this

Table 1
A summary of the evolution of the C_2AH_8 and C_3AH_6 and the parameters for the three-dimensional diffusion kinetics model

Temp. (°C)	C_2AH_8 max.I(s)	C_3AH_6 onset(s)	kt_0	σkt	k (min^{-1})	σk (min)	t_0	R
90	3.2	3.0	0.100	0.005	0.0318	0.00064	3.1	0.99476
85	3.2	3.0	0.094	0.005	0.0281	0.00053	3.3	0.99499
80	3.5	3.5	0.067	0.003	0.0188	0.00025	3.6	0.99630
75	4.0	3.5	0.027	0.002	0.0091	0.00011	2.9	0.99449
70	5.0	4.5	0.012	0.002	0.0074	0.00009	1.7	0.99431
60	9.0	8.0	0.050	0.003	0.0076	0.00009	6.5	0.99719

behaviour was reproducible using different experimental set-ups, and therefore considered to be a real effect.

3.1. Evolution of CA, C_3AH_6, and C_2AH_8

The course of the hydration of CA was systematically scrutinised by plotting α of the hydrates vs. time in the manner explained previously. The diffraction reflections used for this task are summarised in Table 1.

Fig. 4 elucidates the depletion of CA, and the production of C_3AH_6 and C_2AH_8. It can unambiguously be seen that after a certain period, depending on the temperature (the higher the faster), CA suddenly produces C_3AH_6. The transformation is very dramatic. There is no apparent gradual decrease of the CA intensity. Just as the CA begins to hydrate, C_2AH_8 reaches its maximum, which in turn coincides with the onset of C_3AH_6 generation. This sequence of events can be observed at all the temperatures being investigated. Another feature spotted is a slight fluctuation in the CA peak corresponding to an overall change in the background due to the formation of amorphous AH_3 gel. This phase is a natural companion of C_2AH_8 because the chemical balance of the hydration has to be preserved.

The times at which the hydrates appear are summarised in Table 1. At 60°C C_3AH_6 is formed within 8 min. At 70°C the reaction is twice as fast with C_3AH_6 forming in just over 4 min. However, at 90°C, twenty degrees higher, there is no real difference in the time elapsed before starting to produce C_3AH_6.

Additionally, it is noted that once an equilibrium or termination situation is attained, CA reaches a plateau over the background. In other words, some CA

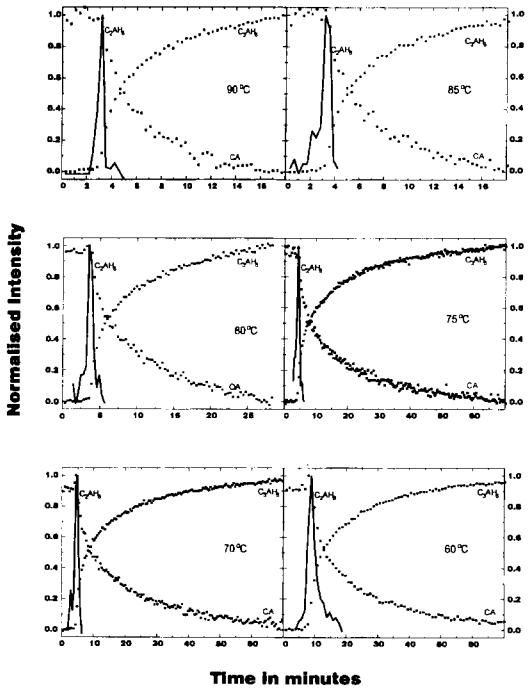

Fig. 4. The hydration of calcium aluminate phases; C_2AH_8 and C_2AH_6 from CA pastes. These have been represented by plotting the main peaks of the phases normalised against time in minutes, the temperature ranging between 60–90°C.

remains unreacted. This is because the amount of water initially used is not sufficient to hydrate all the primary reactant. From the stoichiometric reaction it is easy to calculate that with a w/s of 0.4, 88% of the material can be hydrated, if the full reaction is considered. The sole reason for choosing this w/s ratio is merely that it is the concentration recommended by the manufacturer in order to achieve the best mechanical properties of calcium aluminate systems.

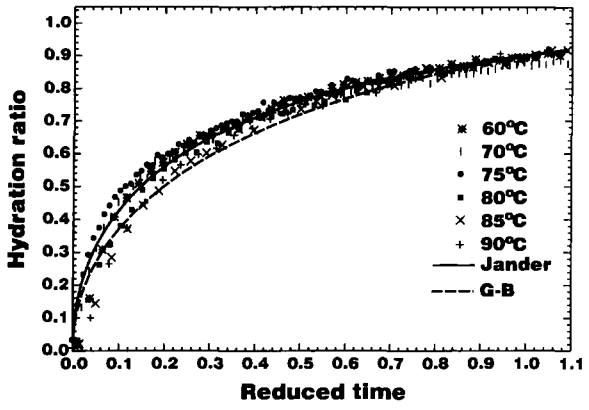

Fig. 5. The formation of C_3AH_6 from CA, at varying temperatures, is presented in reduced time form, where the hydration ratio α is plotted against reduced time.

4. Discussion

4.1. Possible kinetics models

The formation of C_3AH_6 at varying temperatures appears to follow a similar trend. Plots obtained for the range of temperatures studied are assembled in Fig. 5. The shape of the graph for each temperature is comparable and adopts a pseudo-parabolic deceleratory form with minimal deviations.

Out of the three families of deceleratory rate equations encompassing nine different models [12] it was found that *Ginstling–Brounshtein*, two- and three-dimensional diffusion schemes showed the best match. Hence to distinguish from these three types regression analysis was used. This was accomplished by plotting and testing the linearity of the α-dependent part of the equation vs. time, see Table 2 [12].

It was clear that the best fit corresponded to a three-dimensional diffusion mechanism also known as the *Jander* model. The equation complying with a three-dimensional diffusion mechanism is:

$$(1-(1-\alpha)^{1/3})^2 = k(t-t_0), \tag{3}$$

with k being the constant of the reaction and t_0 the dormant period, before the reaction starts to become manifest.

The physical foundations of this model are based on a progressive and homogeneous covering of the solid reactant as the reaction advances. The limiting factor, hence the controlling one, is the diffusion process through the layer of product formed on the surface of the reactant [12].

4.2. The determination of kinetics parameters

To ease the regression analysis by least squares, the data were plotted in the form of $(1-(1-\alpha)^{1/3})^2$ vs. time to obtain straight lines. In Table 1 a recount of the parameters obtained can be found. The second column gives the times at which the C_2AH_8 content attains a maximum and it is computed from the (002) reflection intensity. The third column displays the onset of C_3AH_6, calculated from the profile intensity of the (211) reflection. From the fourth column onwards a summary of the parameters, with their standard deviations, obtained after applying the three-dimensional diffusion model to the hydration of pure CA, is given. The last column states the goodness of the fitting assessed by R.

Table 2
Deceleratory rate equations commonly used in kinetic analyses of isothermal reaction of solids

General type	Mechanism	Equation ($kt =$)
Diffusion model	One-dimensional	α^2
	Two-dimensional	$(1-\alpha)\ln(1-\alpha+\alpha)$
	Three-dimensional	$[1-(1-\alpha)^{1/3}]^2$
	Ginstling–Brounshtein	$[1-(2\alpha/3)]-(1-\alpha)^{2/3}$
Geometric model	Contracting area	$(1-(1-\alpha)^{1/2}$
	Contracting volume	$1-(1-\alpha)^{1/3}$
Order with respect to α^c	First order	$-\ln(1-\alpha)$
	Second order	$(1-\alpha)^{-1}$
	Third order	$(1-\alpha)^{-2}$

As it is expected, the general trend observed in Table 1 indicates that the hydration velocity increases with temperature. This is clearly shown through the reaction constant (k) column with a regular incremental rate. Only at 60°C is the trend broken. The statistical deviation associated with k does not seem to explain this anomaly. The reason is not clear. It could be speculated that around and below this temperature other mechanisms could co-exist or concur with a three-dimensional diffusion.

Another apparent discontinuity is observed in the column corresponding to the dormant period (t_0). At 70°C this period is shorter than anticipated which is due to a slight deviation from the theoretical straight line, close to the origin. If that is taken in account, a more plausible value close to 5 min can be estimated for the dormant period.

In addition, by plotting ln k vs. $1000/T$ between 70°C and 90°C as quoted in Table 1 it is possible to find the activation energy of the reaction. The outcome of the results is shown in Fig. 6.

The points are rather scattered, more than the expected, from their standard deviations. 90°C and 75°C seem to deviate more from a hypothetical straight line. Nevertheless if a figure has to be given for the activation energy it is better to give the one obtained without discarding any point. Although it is worth to compute E_a considering only the supposedly *well-behaved* points. The value obtained from the slope including all five temperatures is

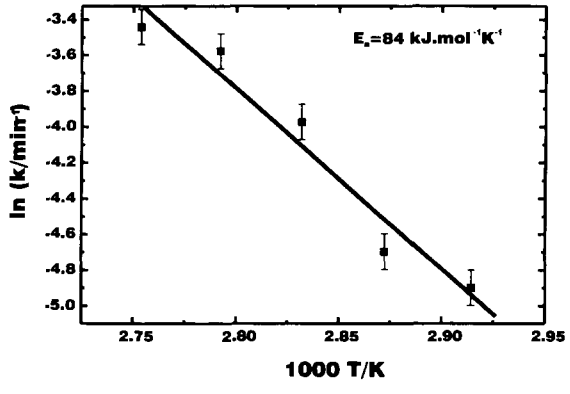

Fig. 6. The logarithmic plot of the reaction constants in the hydration of CA versus the inverse of the absolute temperatures in the range between 70°C and 90°C.

84 kJ mol^{-1} K^{-1}. If two of them are discarded the figure rises to 91 kJ mol^{-1} K^{-1}, still within the 10% bracket of expected error. On the other hand, from the slope between the other two points the activation energy calculated is of the order of 88 kJ mol^{-1} K^{-1}. The implication is that from a statistical point of view the first figure given seems to be faithful, bearing in mind that the error associated to the estimation of activation energies rarely is lower than 10%.

Little more can be said about the activation energy as no other investigations are available for comparative purposes. The only available references are related to dehydration processes. To give an order of magnitude and put the value found in a frame of reference, it will suffice to quote that most of the activation energies range from 50 kJ mol^{-1} K^{-1} to 200 kJ mol^{-1} K^{-1}.

It is clear that the hydration of pure CA seems to follow the *Jander* model. The profiles obtained from 60°C up to 90°C are very similar throughout and follow the model satisfactorily, (see Fig. 5). The essential point is that a diffusion mechanism controls the hydration process in the range of temperatures from 60°C to 90°C.

The diffusing species is the water itself, through a barrier of solid product; C_2AH_8, AH3, C_3AH_6 and gibbsite. Once the water is in contact with the surface of CA more C_3AH_6 is formed. At the beginning the barrier is thin and the water reaches the surface of CA particles with relative ease. But as the layer of product increases it becomes more difficult for the new water molecules to reach the unreacted surface, hence the deceleratory nature of the reaction.

Hence the sequence of events taking place during the hydration can be summarised in the following steps:

1. *Initial contact or wetting* of CA with the water: It happens at room temperature, that is, during mixing, and relates to the process of wetting where the CA particles become coated with water. This step takes place prior to being placed at the temperature of investigation.
2. *Dormant period* of the hydration: The water reacts with CA, at the interface, to produce a layer of very small crystallites of C_2AH_8 (i.e. *germ nuclei*) and AH_3 which are not readily detected by diffraction. The reaction follows according to Eq. (2).

3. *Nucleation period*: As C_2AH_8 crystals become bigger and more established (*grown-up nuclei*), they are easily detected by diffraction and provide the essential nuclei for the formation of C_3AH_6.
4. *Auxiliary conversion* of C_2AH_8 to the more stable cubic hydrate according to the reaction:

$$C_2AH_8 + CA + H \rightarrow C_3AH_6 + AH_3 \quad (4)$$

5. *Principal conversion*: As the water penetrates through the barrier of hydrates and AH_3, further consumption of unhydrated CA directly to C_3AH_6 takes place, as described in the literature according to the Eq. (1)
6. *Completion of the hydration*: This final step includes the ultimate and slowest part of the hydration. Progressively thicker layers of product formed around the CA, make the penetration of water even more difficult and eventually exhaustion occurs because, either no more water is available, or CA has been completely hydrated. In the conditions at which the experiments took place with a w/s ratio of 0.4, it is rather the first premise which is fulfilled, as it has been explained before. Water is the limiting reactant.

A sketch of these events is shown in Fig. 7 which visually describes the reaction of the water with CA to produce C_2AH_8, amorphous AH_3 then C_3AH_6 and gibbsite.

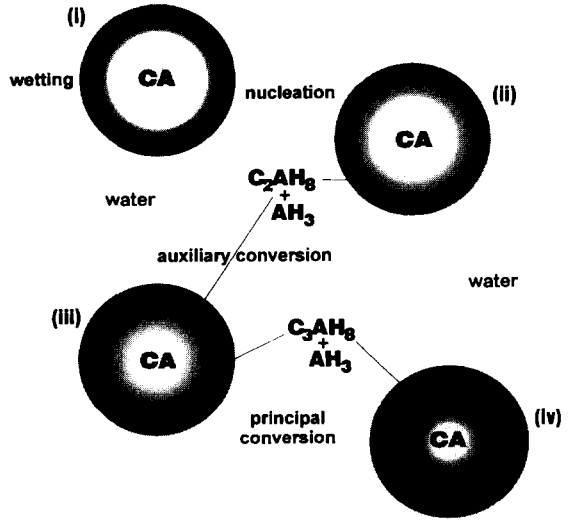

Fig. 7. A schematic representation of the various steps involved during the hydration of CA proposed by the solid-state mechanism.

The suggested hypothesis indicates a solid-state reaction mechanism rather than a through solution one. Although this second model has been widely accepted it has to be noted that no direct experimental evidence, above 50°C, has been given to support it and that all the studies were actually carried out in static equilibrium and dilute conditions [16], somewhat unrelated to the actual conditions in the hydrating calcium aluminate systems.

Another feature to be highlighted is the central protagonism of C_2AH_8 in the whole hydration process. In the range of temperatures investigated, from 60°C to 90°C, this hydrate is the first to emerge, just prior to the onset of C_3AH_6. Its life span is relatively short at 90°C, no longer than 2 min, and just over 10 min at 60°C. This directly indicates that C_2AH_8 is the nucleating agent necessary for the subsequent crystalline growth of C_3AH_6.

The importance of C_2AH_8 resides, not only in the rôle it plays as a trigger of the hydration, but because its conspicuous presence furnishes an argument to discard a through solution mechanism. It is readily admitted that detection of phases by diffraction techniques requires at least a 10% by weight of the diffracting mass. If the mechanism were to be a through solution one, then only 1.43 mg of the total mass used for a typical experiment 0.14% by weight, in accordance with the data provided in [13], would be precipitated. Even if the dissolution/precipitation cycles were to be repeated it is highly unlikely that at least 10% by weight of C_2AH_8 would be precipitated in such short time (within 3 min at 90°C) to give a detectable diffraction pattern. Briefly, C_2AH_8 could not be detected if it was produced by a through solution mechanism. It could be added to reinforce the first hypothesis that a rapid succession of dissolution precipitation cycles would be increasingly difficult as the liquid phase becomes richer in aluminium-ion species hindering even further the solubility of CA.

Furthermore, the present experiments undertaken with synchrotron EDD are not the only ones which suggest a different mechanism to the widely accepted through solution formation. Geßner et al. [14] concluded, from work undertaken at 20°C and 50°C, that CA hydration is characterised by different reaction layers on the unhydrated grain. They went further to

state that the reaction rate is influenced by the permeability of these layers which vary with time, temperature and different conversion–crystallisation processes.

Bushnell-Watson and Sharp working at temperatures between 35°C and 55°C also found the rate determining factor to be nucleation following an Avrami–Erofe'ev kinetics process [15].

By probing further back into the literature similar observations can be found in numerous authors' research. For example, as early as 1953, D'Ans and Eick, as quoted in L'Hopitallier's literature review [17], observed a retarding superficial film at the surface of anhydrous particles. Lea graphically described the reaction of CA with water under the optical microscope, again relating it with the formation of a gelatinous phase and hexagonal plates surrounding the CA grains [18].

Similar findings were noted using microcalorimetry by Magnan [19] who further inferred that the impermeable layer encompassing the unhydrated grain hindered the rate of the hydration reaction, while Fujii et al. [20] working with solutions actually showed that crystallites formed on the surface of the CA particle but not in the liquid phase.

These are just a few examples of what can be found in the literature and therefore the hypothesis proposed has also been supported by the experiments and observations made by other authors.

5. Conclusion

Synchrotron EDD in situ studies of CA hydration carried out at temperatures ranging from 60–90°C have revealed new interesting kinetics aspects.

Quantitative processing of the results, in the form of reduced time graphs, has led to the conclusion that the limiting factor of the hydration is the diffusion of water through a solid barrier. Indeed, the experimental values are in agreement with a three-dimensional diffusion-controlled kinetics model. A solid-state reaction mechanism in five steps has been proposed which implies that the unhydrated spherical particles of CA react at the interface with the water creating a product layer. The hydrates' degree of crystallinity influences the permeability of the layer and hence the overall rate of reaction.

The time scale of the hydration of pure CA has been quantitatively characterised from the fitted kinetics model; the reaction constants range from $7.5 \times 10^{-3}\ \mathrm{min}^{-1}$ at 70°C to $3.2 \times 10^{-2}\ \mathrm{min}^{-1}$, which allows the estimation of an activation energy, for that domain, of 84 kJ $\mathrm{mol}^{-1}\ \mathrm{K}^{-1}$. This value is reasonable although it could not be compared with any from previous studies, as this is the first time quantitative experimental information is reported on the hydration of CA at high temperatures. Therefore, this could be regarded as the starting point for further studies in this area. A possible path to explore could be to see the influence of particle size distribution; being a surface-dependent reaction a larger surface per volume ratio will in principle increase the hydration rate.

Acknowledgements

The authors would like to thank Dr. C.C. Tang, station master of 9.7, for his valuable help and Daresbury Laboratory for the beamtime allocated. Thanks are also extended to Lafarge Aluminates for providing the time and raw materials to undertake the study. The authors also acknowledge Prof. C. Hall from Schlumberger Cambridge Research for kindly using the environmental cell and Prof. P. Barnes from Birkbeck College for the use of the Crystallography Department facilities.

References

[1] S. Mathew, N. Eisenreich and W. Engel, Thermochimica Acta, 269/270 (1995) 475.
[2] P. Barnes, S.M. Clark, D. Häusermann, E. Henderson, C.H. Fentiman, M.N. Muhamad and S. Rashid, Phase Transitions, 39 (1992) 117.
[3] D. Sorrentino, F. Sorrentino and C.M. George Material Science of Concrete, IV (1995) 41.
[4] H.G. Midgley and A. Midgley, Magazine of Concrete Research, 27 (1975) 59.
[5] A. Rettel, W. Geßner, D. Müller and G. Scheler, British Ceramic Transactions Journal, 84 (1985) 25.
[6] S. Rashid, P. Barnes and X. Turrillas, Advances in Cement Research, 4 (1991/1992) 61.
[7] A. Capmas, D. Ménétrier-Sorrentino and D. Damidot, in R.J. Mangabhai (Ed.), Calcium Aluminate Cements, (E and FN Spon, London, 1990), p. 65.
[8] S.M. Clark, Nuclear instruments and methods in physics research, Amsterdam, A279 (1988) 381.

[9] J. Cockcroft, Program RAWSPF PDPL software package, 1994.
[10] X. Turrillas, Birkbeck College Internal Report, 1992.
[11] MicroCal Software Program ORIGIN version 3.0, Technical Graphics and Data Analysis in Windows, Northampton, MA, USA, 1993.
[12] W.E. Brown, D. Dollimore and A.K. Galwey, in C.H. Bamford and C.F.H. Tipper (Eds.), Comprehensive Chemical Kinetics, 22, (Elsevier Scientific, Amsterdam, 1980) p. 74.
[13] P. Barret and D. Bertrandie, International Symposium on Chemistry of Cements, Paris, vol. III, p. V-134 1980.
[14] W. Geßner, R. Trettin, A. Rettel and D. Müller, in R.J. Mangabhai (Ed.), Calcium Aluminate Cements, (E and FN Spon, London, 1990), p. 96.
[15] S.M. Bushnell-Watson and J.H. Sharp, Cement and Concrete Research, 20 (1990) 677.
[16] A. Capmas and D. Ménétrier-Sorrentino, 1st Biennial Worlwide Conference on Refractories, Anaheim, CA, 1989.
[17] P. L'Hopitallier, International Symposium on Chemistry of Cements, Washington DC, Paper VIII-4, 1960.
[18] F.A. Lea, The Chemistry of Cement and Concrete, 3rd edn., (Edward Arnold Ltd., London), 1970.
[19] R. Magnan, Ceramic Bulletin, 49 (1970) 3.
[20] K. Fujii, W. Kondo and H. Ueno, Journal of American Ceramic society, 69 (1986) 361.